Correlation between CT numbers and tissue parameters needed for Monte Carlo simulations of clinical dose distributions

2000 Phys. Med. Biol. 45 459

(http://iopscience.iop.org/0031-9155/45/2/314)

Phys. Med. Biol. **45** (2000) 459–478. Printed in the UK PII: S0031-9155(00)00140-8

Correlation between CT numbers and tissue parameters needed for Monte Carlo simulations of clinical dose distributions

Wilfried Schneider, Thomas Bortfeld and Wolfgang Schlegel

Department of Medical Physics, Deutsches Krebsforschungszentrum, Im Neuenheimer Feld 280, 69120 Heidelberg, Germany

Received 14 December 1998, in final form 17 November 1999

Abstract. We describe a new method to convert CT numbers into mass density and elemental weights of tissues required as input for dose calculations with Monte Carlo codes such as EGS4. As a first step, we calculate the CT numbers for 71 human tissues. To reduce the effort for the necessary fits of the CT numbers to mass density and elemental weights, we establish four sections on the CT number scale, each confined by selected tissues. Within each section, the mass density and elemental weights of the selected tissues are interpolated. For this purpose, functional relationships between the CT number and each of the tissue parameters, valid for media which are composed of only two components in varying proportions, are derived. Compared with conventional data fits, no loss of accuracy is accepted when using the interpolation functions. Assuming plausible values for the deviations of calculated and measured CT numbers, the mass density can be determined with an accuracy better than 0.04 g cm^{-3}. The weights of phosphorus and calcium can be determined with maximum uncertainties of 1 or 2.3 percentage points (pp) respectively. Similar values can be achieved for hydrogen (0.8 pp) and nitrogen (3 pp). For carbon and oxygen weights, errors up to 14 pp can occur. The influence of the elemental weights on the results of Monte Carlo dose calculations is investigated and discussed.

1. Introduction

Clinical dose distributions can be significantly influenced by tissue inhomogeneities. Owing to this fact, as early as 1974 dose calculations were being corrected for inhomogeneities in the computerized planning process for photon therapy (Milan and Bentley 1974). However, not until the availability of computed tomography (CT) could such correction methods be used accurately in radiotherapy treatment planning. This is for two reasons. First, the CT scans provide the exact anatomical location of the inhomogeneities, and second, the CT number includes quantitative information about the radiological properties of the different tissues. Because the CT scans are taken at x-ray energies of about 100 keV, the radiological properties relative to the beam quality used in therapy (high-energy photons and electrons, protons, heavy ions) are not directly available and must be obtained by conversion of the CT number. For photons, first approaches in this direction were made by Kijewski and Bjärngard (1978) and Parker *et al* (1979). The latter have established a relationship between CT number and electron density of the tissues. This approximation can be used for photon therapy, provided that the Compton process is the predominant interaction. Henson and Fox (1984) have improved the relationship from Parker *et al* for skeletal tissues. In the pencil beam algorithm for electron dose calculation by Hogstrom *et al* (1981) the CT number is correlated with the collision stopping

0031-9155/00/020459+20$30.00

power and the scattering power of the tissues. The more sophisticated electron dose calculation algorithm VMC (Kawrakow *et al* 1996) in addition makes use of the radiation stopping power of the tissues. Schneider *et al* (1996) have established a stoichiometric calibration of the CT number with the proton stopping power as well as with the electron density. The problem of correlating the CT number with the water equivalent pathlength needed for dose calculation in heavy ion therapy was solved by Jacob (1997).

Whenever the dose calculation is done by direct simulation of the interactions between the radiation and the patient tissue, the mass density and the chemical composition of the tissues are needed for the precalculation of the physical cross sections. An example for a dose calculation tool of this type is the Monte Carlo code for electrons and photons, EGS4 (Nelson *et al* 1985). Applications of the Monte Carlo method for patient dose calculations have recently become more and more common (Wang *et al* 1998, DeMarco *et al* 1998, Hartmann Siantar *et al* 1997, Gao and Raeside 1997, Manfredotti *et al* 1990). To correlate the CT number with the elemental weights of the tissues, all of these authors have defined threshold values dividing the scale of CT numbers into different groups. Within each group, the values for the elemental weights are then constant. The maximum number of groups was realized by DeMarco *et al*, who have defined the media air, lung, fat, water, muscle and bone. The respective chemical compositions were taken from the literature. To consider the variation of the mass density with the CT number, they used a calibration curve, which was measured on the individual CT scanner.

Concerning this method of converting the CT number into tissue parameters, two questions arise. First, no rule is given by the authors about how to determine the threshold values correctly. The second point is that none of them proved whether the raw classification into a few different media is sufficient for the task of clinical Monte Carlo dose calculations. For the special case of an 8 MV photon beam, the influence of the different body tissues on the dose distributions is investigated by du Plessis *et al* (1998). Considering 16 main body tissues, they combined all those tissues within subsets, which are dosimetrically equivalent with respect to a clinical 8 MV photon beam. In the Monte Carlo simulation, each subset is then represented by the tissue parameters of an arbitrary member. The authors have found that seven subsets are sufficient to obtain an accuracy of 1% in the calculated dose distribution. In the range of skeletal and lung tissue, a further classification of the mass density within the subsets was necessary to fulfil this level of accuracy. The CT threshold values defining the subsets are determined using an electron density calibration curve measured on the CT scanner.

The disadvantage of the method of du Plessis *et al* is that the application of the resulting conversion of CT number into tissue parameters is limited to the special beam quality under consideration. In this paper, we describe an alternative way. Our investigations are focused to extract more information about the tissue parameters from the CT number irrespective of the therapeutic beam quality. We present a method for a stoichiometric calibration of the CT number with the mass density and the elemental weights. The method is applied to a CT scanner of the type Siemens Somatom Plus 4. The resulting conversion of CT numbers is presented and discussed.

2. Methods and materials

2.1. X-ray attenuation coefficient and CT number

The imaging in a computed tomography (CT) scanner is done by measuring projected transmission profiles of x-rays penetrating a patient from different directions. By means of a reconstruction method, the projection values can be transformed into a series of cross-sectional

images of the patient. A detailed description of the principles of CT is given in Kak and Slaney (1988). In the following only the quantities used in this paper are described. The attenuation of x-rays with a typical mean energy of 50–100 keV is determined by three different physical processes: photoelectric absorption (σ^{ph}), coherent scattering (Rayleigh process σ^{coh}) and incoherent scattering (Compton process σ^{icoh}). Depending on the detector system of the CT scanner, the measured signal S will be either proportional to the particle fluence, to the energy fluence, or, if the detector is an ionization chamber, to the energy deposition per mass. Due to the fact that there is a polychromatic spectrum of x-rays, the measured signal S must be described by an integral of the form

$$S \propto \int f(E)\,\mathrm{d}E. \tag{1}$$

In the case that the particle fluence is measured, $f(E)$ is proportional to the product of the particle fluence per energy interval $\Phi_E(E)$ and to the detector sensitivity. If the energy fluence or the energy deposition is measured, $f(E)$ is additionally proportional to the particle energy or to the product of particle energy and mass energy absorption coefficient (McCullough 1975).

If the initial particle fluence of the x-rays is given by $\Phi_{E,0}(E)$, the particle fluence of the transmitted x-rays entering the detector behind the patient will be

$$\Phi_E(E) = \Phi_{E,0}(E) \exp\left(-\int_0^s \mu(E,t)\,\mathrm{d}t \right). \tag{2}$$

In this formula, $\mu(E,t)$ is the linear attenuation coefficient of the tissue at position t along the projection line with length s

$$\mu(E) = \rho N_{\mathrm{A}} \sum_{i=1}^{n} \left(\frac{w_i}{A_i} \sigma_i(E) \right) \tag{3}$$

with ρ (g cm^{-3}) the mass density, N_{A} (mol^{-1}) the Avogadro constant ($6.022\,045 \times 10^{23}$), i the element index, w_i the elemental weight, σ_i (barn/atom) the total cross section $\sigma_i^{\mathrm{icoh}} + \sigma_i^{\mathrm{coh}} + \sigma_i^{\mathrm{ph}}$ and A_i (g mol^{-1}) the atomic mass. The measured detector signals are analysed in such way that projection values λ are calculated as the logarithmic ratio of the signal measured without a patient in the CT scanner and the signal of the x-rays attenuated by the patient, i.e. $\lambda = \ln(S_0/S)$. In the case of monochromatic x-rays we get

$$\lambda = \ln\left(\frac{\Phi_0}{\Phi} \right) = \int_0^s \mu(E,t)\,\mathrm{d}t. \tag{4}$$

Reconstructing these line integrals would give the values $\mu(E)$ of the different tissues, i.e. a well defined physical quantity. For the case of polychromatic x-rays, one could assume that the reconstructed attenuation values are mean values according to the spectral function $f(E)$. Unfortunately, the attenuation value of one and the same tissue depends on the location within the patient. This effect is caused by beam hardening: the energy spectrum of a polychromatic x-ray is shifted towards higher energies while penetrating a medium, because the physical cross sections are bigger for low-energy photons. On state-of-the-art CT scanners, this disturbing effect can be eliminated to a high degree by correcting the projection value λ of each line integral. In the following, we will assume that the reconstructed attenuation values of the different tissues are completely independent of the location of the tissues. The attenuation values can then be considered as mean values $\bar{\mu}$ according to a location independent spectral function $\hat{f}(E)$:

$$\bar{\mu}(s) = \frac{\int \hat{f}(E)\mu(E,s)\,\mathrm{d}E}{\int \hat{f}(E)\,\mathrm{d}E}. \tag{5}$$

To obtain comparable attenuation values for different CT scanners, the values of $\bar{\mu}$ are converted into Hounsfield units H:

$$H = \left(\frac{\bar{\mu}}{\bar{\mu}_{H_2O}} - 1 \right) 1000. \tag{6}$$

This CT number is defined in such way that water has always the value 0 and air the value -1000. It has to be mentioned that the ratio of $(\bar{\mu}/\bar{\mu}_{H_2O})$ also slightly depends on the spectral function $\hat{f}(E)$ and therefore the CT number is a scanner-dependent quantity with fixed values for water and air.

Our task is now to convert the Hounsfield units of the patient's CT data into the mass density and chemical composition of human tissues. It can be seen that equations (3), (5) and (6) together indeed establish a functional relationship between the desired tissue parameters (ρ, w_i) and the Hounsfield units H. However, apart from the problem that the spectral function $\hat{f}(E)$ of the CT scanner is normally unknown, different sets of tissue parameters are related with the same CT number. To illustrate this in more detail, figure 1 shows a projection of the space of tissue parameters. In this presentation, the ordinate value

$$\frac{1}{\bar{\mu}_{H_2O}} \frac{\bar{\mu}}{\rho} = \frac{1}{\bar{\mu}_{H_2O}} N_A \sum_{i=1}^{n} \left(\frac{w_i}{A_i} \bar{\sigma}_i \right) \tag{7}$$

is determined by the elemental weights w_i and is independent of the mass density ρ, which is denoted along the abscissa. The hyperbolas drawn in the figure mark the lines with constant CT number. The information provided by the CT data is therefore restricted to determining the hyperbola that represents the tissue in question. Tissues with different mass density and elemental weights, but represented by the same hyperbola, cannot be resolved with the CT scanner. Fortunately, not all sections along the hyperbolas are correlated with meaningful values for the tissue parameters. Hence the strategy must be to determine those areas in the parameter space that are indeed represented by the human tissues. For this, we have to calculate for all tissues the CT number, which corresponds to our special CT scanner. The method we apply for this task is the same as used by Schneider *et al* (1996). These authors have calculated CT numbers of tissues for a stoichiometric calibration of CT data with proton stopping power and electron density. Note that our notation is different from that used by Schneider *et al* (1996).

2.2. Calculation of the CT number of human tissues

As already mentioned above, a direct calculation of the CT number using equations (3), (5) and (6) together with tabulated values for the cross sections σ is not possible because the spectral function $\hat{f}(E)$ is unknown. However, as shown by Rutherford *et al* (1976), for the range of diagnostic x-ray energies and the elements contained in human tissues, the following parametrization of the cross section can be used in good approximation:

$$\sigma_i(E) = Z_i K^{KN}(E) + Z_i^{2.86} K^{sca}(E) + Z_i^{4.62} K^{ph}(E). \tag{8}$$

In the first term of this formula, K^{KN} denotes the Klein–Nishina coefficient. The coherent scattering as well as the binding correction for the incoherent scattering are described by the second term, and the photoelectric absorption is taken into account by the third term. If $\sigma_i(E)$ is eliminated in equation (3) by this expression, the mean value of the attenuation coefficient will be

$$\bar{\mu} = \rho N_A \sum_{i=1}^{n} \left(\frac{w_i}{A_i} (Z_i \bar{K}^{KN} + Z_i^{2.86} \bar{K}^{sca} + Z_i^{4.62} \bar{K}^{ph}) \right). \tag{9}$$

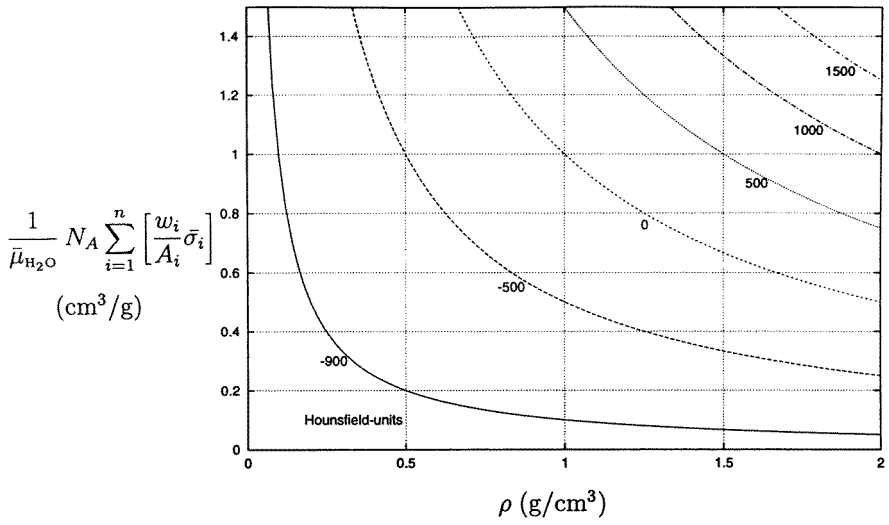

Figure 1. Coordinate system to represent the tissue parameters (ρ, w_i). Note that the ordinate value is equal to $(\bar{\mu}/\bar{\mu}_{H_2O})(1/\rho)$. The hyperbolas with the mathematical form (const/ρ) therefore depict the areas of parameters which lead to the same CT number.

The coefficients $(\bar{K}^{KN}, \bar{K}^{sca}, \bar{K}^{ph})$ are mean values with respect to the spectral function $\hat{f}(E)$. For the attenuation relative to water one gets

$$\frac{\bar{\mu}}{\bar{\mu}_{H_2O}} = \frac{\rho}{\rho_{H_2O}} \frac{\sum_{i=1}^{n}(w_i/A_i)(Z_i + Z_i^{2.86}k_1 + Z_i^{4.62}k_2)}{(w_H/A_H)(1 + k_1 + k_2) + (w_O/A_O)(8 + 8^{2.86}k_1 + 8^{4.62}k_2)} \tag{10}$$

with

$$k_1 \equiv \frac{\bar{K}^{sca}}{\bar{K}^{KN}} \qquad k_2 \equiv \frac{\bar{K}^{ph}}{\bar{K}^{KN}}.$$

The values of (k_1, k_2) are dependent on the CT scanner and are determined experimentally according to the following procedure. First, for the 16 phantom materials listed in table 1 the CT numbers are measured in the scanner (Jacob 1997). Then, we determine the values of (k_1, k_2) by carrying out a least square fit of the measured CT numbers to equation (10), i.e. the expression

$$\sum_{n=1}^{16}\left[\left(\frac{\bar{\mu}}{\bar{\mu}_{H_2O}}(k_1, k_2)\right)_n - \left(\frac{H(\text{meas.})}{1000} + 1\right)_n\right]^2 \tag{11}$$

is minimized. The resulting values are $k_1 = 1.24 \times 10^{-3}$ and $k_2 = 3.06 \times 10^{-5}$. Table 2 lists the measured and calculated CT numbers of the phantom materials. A graphical presentation of the fit result is shown in figure 2.

By means of equations (6) and (10) together with the above values of (k_1, k_2) we have calculated the CT numbers of 71 human tissues, whose mass densities and elemental weights are taken from the literature (White *et al* 1987, Woodard and White 1986). They are listed in tables 3–5. If we look at the spectrum of human tissues, we can see that the soft tissues are situated within the range between −100 and +100 Hounsfield units, whereas the CT numbers of the skeletal tissues take values from 100 up to 1524. A graphical presentation of the 71 human tissues in the parameter space is shown in figure 3. In the range between −100 and 0 Hounsfield units, as well as in the range of skeletal tissues, the data points are aligned mostly in

Table 1. Mass-density and chemical composition of the 16 phantom materials used for the determination of k_1 and k_2 values.

Phantom material	Density ρ (g cm^{-3})	Elemental weights in percentage points (pp)									
		H	C	N	O	Mg	Si	Cl	Ca	Ti	Sn
Compact bone	1.84	3.1	31.26	0.99	37.57			0.05	27.03		
Muscle	1.05	8.1	67.17	2.42	19.85			0.14	2.32		
Fat	0.92	8.5	72.88	2.24	16.25			0.13			
Lung	0.3	8.36	60.43	1.67	17.33	11.36	0.72	0.13			
Spongiosa	1.14	7.9	63.79	4.23	9.88				14.2		
Solid Water	1.035	8.09	67.22	2.4	19.84			0.13	2.32		
RW − 3	1.045	7.59	90.41		0.8					1.2	
H − 800	0.23	7.96	64.21		16.29		11.48				0.06
H − 500	0.47	8.04	45.93		19.41		26.48				0.14
H + 200	1.04	7.7	31.5		22.99		35.66		1.96		0.19
H + 400	1.12	6.35	28.07		27.38		29.4		8.64		0.16
H + 700	1.36	4.59	23.63		33.09		21.28		17.33		0.06
H + 900	1.43	3.72	21.41		35.93		17.21		21.64		0.09
H + 1200	1.65	2.4	18.07		40.21		11.1		28.16		0.06
PMMA	1.19	8.0	60.0		32.0						
Polyethylene	0.94	14.4	85.6								

Table 2. CT numbers of the phantom materials from table 1. The values H(meas.) are measured on a Siemens Somatom Plus 4 CT scanner with a tube voltage of 120 kV (Jacob 1997). The values H(calc.) are calculated by means of equation (10) with values $k_1 = 1.24 \times 10^{-3}$ and $k_2 = 3.06 \times 10^{-5}$. In the last column is listed the difference of the measured and calculated Hounsfield units.

ID	Phantom material	H(meas.)	H(calc.)	ΔH
1	Compact bone	1454 ± 35	1430	24
2	Muscle	41 ± 5	26	15
3	Fat	-108 ± 4	−132	24
4	Lung	-750 ± 19	−708	−42
5	Spongiosa	262 ± 9	311	−49
6	Solid Water	32 ± 4	12	20
07	RW − 3	-3 ± 5	−8	5
8	H − 800	-798 ± 11	−768	−30
9	H − 500	-485 ± 10	−482	−3
10	H + 200	227 ± 10	234	−7
11	H + 400	420 ± 15	392	28
12	H + 700	792 ± 25	763	29
13	H + 900	962 ± 35	927	35
14	H + 1200	1250 ± 65	1312	−62
15	PMMA	138 ± 7	126	12
16	Polyethylene	-84 ± 4	−80	−4

a direction orthogonal to the hyperbolas. The consequence is that those tissues can be resolved to a high degree by means of the CT number. However, in the range between 0 and 100 Hounsfield units, the tissues are also aligned tangential to the hyberbolas, i.e. they can only be poorly distinguished by means of the CT number. To find a correlation between Hounsfield units and the tissue parameters, the data base given by the 71 human tissues could be used directly to carry out fits of the data points (H, ρ) and (H, w_i); i.e. a separate fit procedure

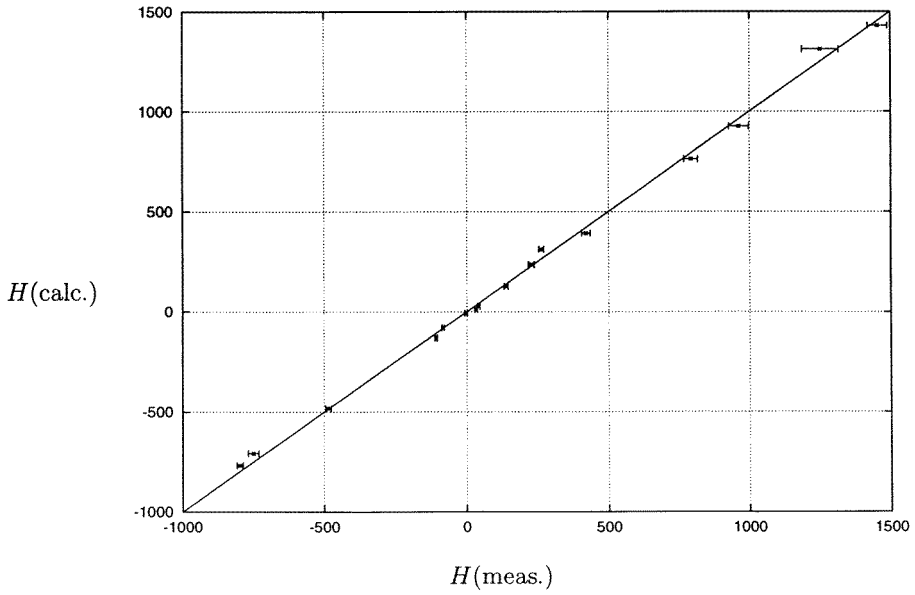

Figure 2. Calculated versus measured Hounsfield units of the phantom materials (values listed in table 2). The straight line represents the ideal case of $H(\text{calc.}) \equiv H(\text{meas.})$.

for each tissue parameter. Because this seems to be a tedious task, we have searched for an alternative way, which is described in the next section.

2.3. Parameter reduced data fits of Hounsfield units to tissue parameters using interpolation functions

All skeletal tissues are composed of bone marrow and osseous tissue in different proportions (Woodard and White 1982). Exceptions are only the few tissues composed of cartilage, e.g. the intervertebral discs. We are therefore able to reduce considerably the amount of tissue data used for the fit process, if we represent the different skeletal tissues by means of their proportions by weight of osseous tissue and bone marrow. Furthermore, it is possible to interpolate the mass density and elemental weights of osseous tissue and bone marrow within the range of Hounsfield units confined by them. In the following, we derive the mathematical relationships between the CT number and the tissue parameters. These formulae are generally valid for all media, which are composed of only two components. The data sets of the components are denoted by $(\rho_1, w_{1,i}, H_1)$ and $(\rho_2, w_{2,i}, H_2)$, that for the composed media by (ρ, w_i, H). We will assign the components such that $H_1 < H_2$. Additionally we use the variable W_1 to denote the proportion of the first component; the proportion of the second component is given by $W_2 = 1 - W_1$. A special value of W_1 defines a medium with the elemental weights

$$w_i = W_1 w_{1,i} + W_2 w_{2,i} = W_1(w_{1,i} - w_{2,i}) + w_{2,i} \tag{12}$$

and the mass density

$$\begin{aligned} \rho &= \frac{m}{V} \\ &= \frac{m}{m_1/\rho_1 + m_2/\rho_2} = \frac{1}{W_1/\rho_1 + W_2/\rho_2} = \frac{\rho_1\rho_2}{W_1(\rho_2 - \rho_1) + \rho_1}. \end{aligned} \tag{13}$$

Table 3. Calculated CT numbers, mass-density and elemental weights of soft tissues. The tissue parameters are taken from Woodard and White (1986), the Hounsfield units are calculated using equations (6) and (10). In the column 'others' are combined the elements Na, Mg, S, Cl, K and Fe.

			w_i (pp)						
Soft tissue	H	ρ (g cm^{-3})	H	C	N	O	P	Ca	Others
Lung, blood-filled	−741	0.26	10.3	10.5	3.1	74.9	0.2		1.0
Adipose tissue 3	−98	0.93	11.6	68.1	0.2	19.8			0.3
Adipose tissue 2	−77	0.95	11.4	59.8	0.7	27.8			0.3
Adipose tissue 1	−55	0.97	11.2	51.7	1.3	35.5			0.3
Mammary gland 1	−37	0.99	10.9	50.6	2.3	35.8	0.1		0.3
Mammary gland 2	−1	1.02	10.6	33.2	3.0	52.8	0.1		0.3
Brain, cerebrospinal fluid	13	1.01	11.1			88.0			0.9
Adrenal gland	14	1.03	10.6	28.4	2.6	57.8	0.1		0.5
Small intestine (wall)	23	1.03	10.6	11.5	2.2	75.1	0.1		0.5
Urine	26	1.02	11.0	0.5	1.0	86.2	0.1		1.2
Gallbladder bile	27	1.03	10.8	6.1	0.1	82.2			0.8
Lymph	29	1.03	10.8	4.1	1.1	83.2			0.8
Pancreas	32	1.04	10.6	16.9	2.2	69.4	0.2		0.7
Prostate	34	1.04	10.5	8.9	2.5	77.4	0.1		0.6
Brain, white matter	34	1.04	10.6	19.4	2.5	66.1	0.4		1.0
Testis	36	1.04	10.6	9.9	2.0	76.6	0.1		0.8
Brain, grey matter	40	1.04	10.7	9.5	1.8	76.7	0.3		1.0
Muscle, skeletal 1	40	1.05	10.1	17.1	3.6	68.1	0.2		0.9
Stomach	41	1.05	10.4	13.9	2.9	72.1	0.1		0.6
Heart 1	41	1.05	10.3	17.5	3.1	68.1	0.2		0.8
Kidney 1	41	1.05	10.2	16.0	3.4	69.3	0.2	0.1	0.8
Thyroid	42	1.05	10.4	11.9	2.4	74.5	0.1		0.7
Aorta	43	1.05	9.9	14.7	4.2	69.8	0.4	0.4	0.6
Heart 2	43	1.05	10.4	13.9	2.9	71.8	0.2		0.8
Kidney 2	43	1.05	10.3	13.2	3.0	72.4	0.2	0.1	0.8
Liver 1	43	1.05	10.3	15.6	2.7	70.1	0.3		1.0
Muscle, skeletal 2	43	1.05	10.2	14.3	3.4	71.0	0.2		0.9
Muscle, skeletal 3	44	1.05	10.2	11.2	3.0	74.5	0.2		0.9
Heart 3	45	1.05	10.4	10.3	2.7	75.6	0.2		0.8
Mammary gland 3	45	1.06	10.2	15.8	3.7	69.8	0.1		0.4
Kidney 3	46	1.05	10.4	10.6	2.7	75.2	0.2	0.1	0.8
Ovary	46	1.05	10.5	9.3	2.4	76.8	0.2		0.8

If we substitute in the expression for the attenuation coefficient of the media

$$\bar{\mu} = \rho N_{\mathrm{A}} \sum_{i=1}^{n} \left(\frac{w_i}{A_i} \bar{\sigma}_i \right) \tag{14}$$

the mass density ρ and the elemental weights w_i by equations (12) and (13), we get

$$\begin{aligned} \bar{\mu} &= \frac{\rho_1 \rho_2}{W_1(\rho_2 - \rho_1) + \rho_1} N_{\mathrm{A}} \left[W_1 \sum_i \left(\frac{w_{1,i} - w_{2,i}}{A_i} \bar{\sigma}_i \right) + \sum_i \left(\frac{w_{2,i}}{A_i} \bar{\sigma}_i \right) \right] \\ &= \frac{\rho_1 \rho_2}{W_1(\rho_2 - \rho_1) + \rho_1} \left[W_1 \left(\frac{\bar{\mu}_1}{\rho_1} - \frac{\bar{\mu}_2}{\rho_2} \right) + \frac{\bar{\mu}_2}{\rho_2} \right]. \end{aligned} \tag{15}$$

After some straightforward transformations and the use of equation (6), we get the following relationship between the weight of the first component W_1 and the Hounsfield units H of the

Table 4. Calculated CT numbers, mass-density and elemental weights of soft tissues. The tissue parameters are taken from Woodard and White (1986), the Hounsfield units are calculated using equations (6) and (10). In the column 'others' are combined the elements Na, Mg, S, Cl, K and Fe.

			w_i (pp)						
Soft tissue	H	ρ (g cm^{-3})	H	C	N	O	P	Ca	Others
Eye, lens	49	1.07	9.6	19.5	5.7	64.6	0.1		0.5
Liver 2	53	1.06	10.2	13.9	3.0	71.6	0.3		1.0
Trachea	54	1.06	10.1	13.9	3.3	71.3	0.4		1.0
Spleen	54	1.06	10.3	11.3	3.2	74.1	0.3		0.8
Heart, blood filled	56	1.06	10.3	12.1	3.2	73.4	0.1		0.9
Blood, whole	56	1.06	10.2	11.0	3.3	74.5	0.1		0.9
Liver 3	63	1.07	10.1	12.6	3.3	72.7	0.3		1.0
Skin 1	72	1.09	10.0	25.0	4.6	59.4	0.1		0.9
Skin 2	74	1.09	10.0	20.4	4.2	64.5	0.1		0.8
Skin 3	77	1.09	10.1	15.8	3.7	69.5	0.1		0.8
Connective tissue	100	1.12	9.4	20.7	6.2	62.2			1.5

composed tissue:

$$W_1 = \frac{\rho_1(H_2 - H)}{(\rho_1 H_2 - \rho_2 H_1) + (\rho_2 - \rho_1)H}. \tag{16}$$

The last step is to substitute W_1 in equations (12) and (13). The resulting relationship between the tissue parameters and the CT number for the composed medium is then given by

$$\rho = \frac{\rho_1 H_2 - \rho_2 H_1 + (\rho_2 - \rho_1)H}{H_2 - H_1} \tag{17}$$

$$w_i = \frac{\rho_1(H_2 - H)}{(\rho_1 H_2 - \rho_2 H_1) + (\rho_2 - \rho_1)H}\left(w_{1,i} - w_{2,i}\right) + w_{2,i} \tag{18}$$

with

$$H_1 \leqslant H \leqslant H_2.$$

Note that for each of the tissue parameters (ρ, w_i) there exists a separate function. Therefore, from the CT number of a medium composed of two known components, we are able to determine in an unambiguous way its density and elemental weights.

If we want to apply these formulae to the range of skeletal tissues, we need the data sets for bone marrow and osseous tissue. The latter component corresponds to the tissue, skeleton, cortical bone, ($H = 1524$), whose mass density and elemental weights are listed in table 5. For the former component, which can be of the tissue type yellow marrow ($H = -49$) or red marrow ($H = 11$), we take the data set of a (1:1) mixture of both types ($H = -22$).

Unfortunately, for the range of soft tissues, such simple relationships between CT number and tissue parameters do not exist, because these tissues are mainly composed of three components (water, fat, protein) rather than of two. Nevertheless, we also try to apply the interpolation method in the range of soft tissues. For this, we have plotted in figure 4 the contents of water and fat in soft tissues versus the CT number. The division into two parts is obvious here. In the left part, the proportion of fat is monotonically decreasing with increasing CT number. This range is confined by adipose tissue 3 ($H = -98$; fat = 87 pp) and adrenal gland ($H = 14$; fat = 26 pp). We interpolate the mass density and elemental weights of these two tissues to fit the data points within the range. Above 13 Hounsfield units, the tissues have a high proportion of water, of minimum 59 percentage points. Although the content of water

Table 5. Calculated CT numbers, mass-density and elemental weights of skeletal tissues. The tissue parameters are taken from White *et al* (1987) and Woodard and White (1986), the Hounsfield units are calculated using equations (6) and (10). In the column 'others' are combined the elements Na, Mg, S, Cl, K and Fe.

			w_i (pp)						
Skeletal tissue	H	ρ (g cm^{-3})	H	C	N	O	P	Ca	Others
Yellow marrow	−49	0.98	11.5	64.4	0.7	23.1			0.3
Yellow/red marrow (1:1)	−22	1.00	11.0	52.9	2.1	33.5	0.1		0.4
Red marrow	11	1.03	10.5	41.4	3.4	43.9	0.1		0.7
Cartilage	102	1.1	9.6	9.9	2.2	74.4	2.2		1.7
Sternum	385	1.25	7.8	31.6	3.7	43.8	4.0	8.5	0.6
Sacrum (male)	454	1.29	7.4	30.2	3.7	43.8	4.5	9.8	0.6
D6, L3 incl. cartilage (male)	466	1.3	7.3	26.5	3.6	47.3	4.8	9.8	0.7
Whole vertebral column (male)	514	1.33	7.1	25.8	3.6	47.2	5.1	10.5	0.7
D6, L3 excl. cartilage (male)	526	1.33	7.0	28.7	3.8	43.7	5.1	11.1	0.6
Humerus, spherical head	538	1.33	7.1	37.9	2.6	34.2	5.6	12.2	0.4
Femur, spherical head	538	1.33	7.1	37.9	2.6	34.2	5.6	12.2	0.4
Femur, conical trochanter	586	1.36	6.9	36.6	2.7	34.7	5.9	12.8	0.4
C4 incl. cartilage (male)	599	1.38	6.6	24.3	3.7	47.1	5.7	11.9	0.7
Sacrum (female)	621	1.39	6.6	27.1	3.8	43.5	5.8	12.5	0.7
Humerus, whole specimen	636	1.39	6.7	35.2	2.8	35.2	6.2	13.5	0.4
Ribs 2nd, 6th (male)	657	1.41	6.4	26.3	3.9	43.6	6.0	13.1	0.7
Innominate (male)	658	1.41	6.3	26.2	3.9	43.6	6.1	13.2	0.7
C4 excl. cartilage (male)	672	1.42	6.3	26.1	3.9	43.6	6.1	13.3	0.7
Femur (total bone)	688	1.42	6.3	33.3	2.9	36.2	6.6	14.3	0.4
Femur (whole specimen)	702	1.43	6.3	33.1	2.9	36.3	6.6	14.4	0.4
Innominate (female)	742	1.46	6.0	25.0	3.9	43.5	6.6	14.3	0.7
Clavicle, scapula	756	1.46	6.0	31.3	3.1	37.0	7.0	15.2	0.4
Humerus (total bone)	756	1.46	6.0	31.4	3.1	36.9	7.0	15.2	0.4
Humerus, cylindrical shaft	805	1.49	5.8	30.1	3.2	37.4	7.2	15.8	0.5
Ribs 10th (male)	843	1.52	5.6	23.5	4.0	43.4	7.2	15.6	0.7
Cranium	999	1.61	5.0	21.2	4.0	43.5	8.1	17.6	0.6
Mandible	1113	1.68	4.6	19.9	4.1	43.5	8.6	18.7	0.6
Femur, cylindrical shaft	1239	1.75	4.2	20.4	3.8	41.5	9.3	20.2	0.6
Cortical bone	1524	1.92	3.4	15.5	4.2	43.5	10.3	22.5	0.6

varies by up to 20 pp between tissues with nearly the same CT number, a global decrease in the proportion of water with increasing Hounsfield units can be clearly seen. To fit the data points of the 35 soft tissues in this range, we interpolate the tissue parameters of small intestine (wall) ($H = 23$; water = 81 pp) and connective tissue ($H = 100$; water = 60 pp).

3. Results

3.1. Data fit in the range of skeletal tissues

If we enter the data sets of skeleton cortical bone (cb) and red/yellow marrow (ma) into equations (17) and (18), we obtain the following functions for the conversion of the CT number into the mass density and the elemental weights:

$$\rho = (1.017 + 0.592 \times 10^{-3} H) \text{ g cm}^{-3} \tag{19}$$

$$w_i = \frac{1524 - H}{1566 + 0.92H}(w_{\text{ma},i} - w_{\text{cb},i}) + w_{\text{cb},i} \tag{20}$$

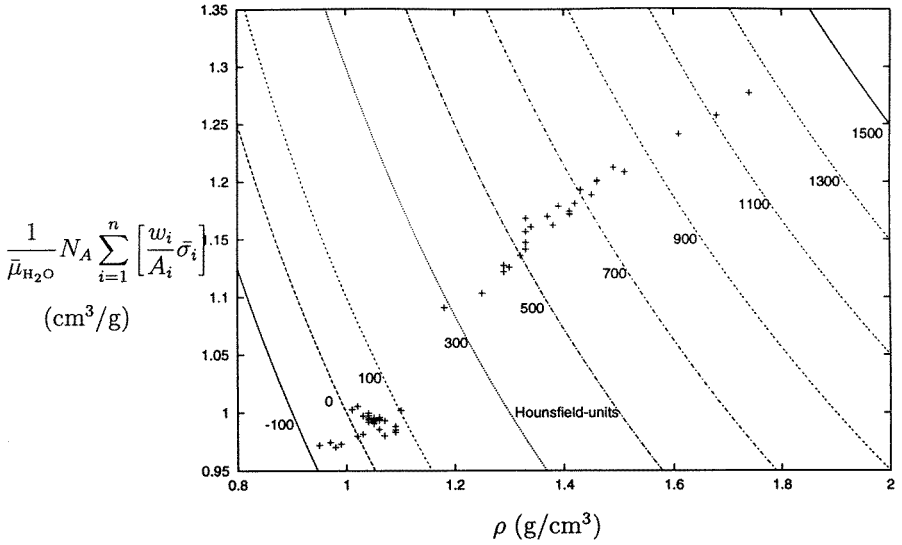

Figure 3. Projection of the space of tissue parameters (ρ, w_i). The data points are corresponding to the 71 human tissues. Along the hyperbolas, the CT number is constant.

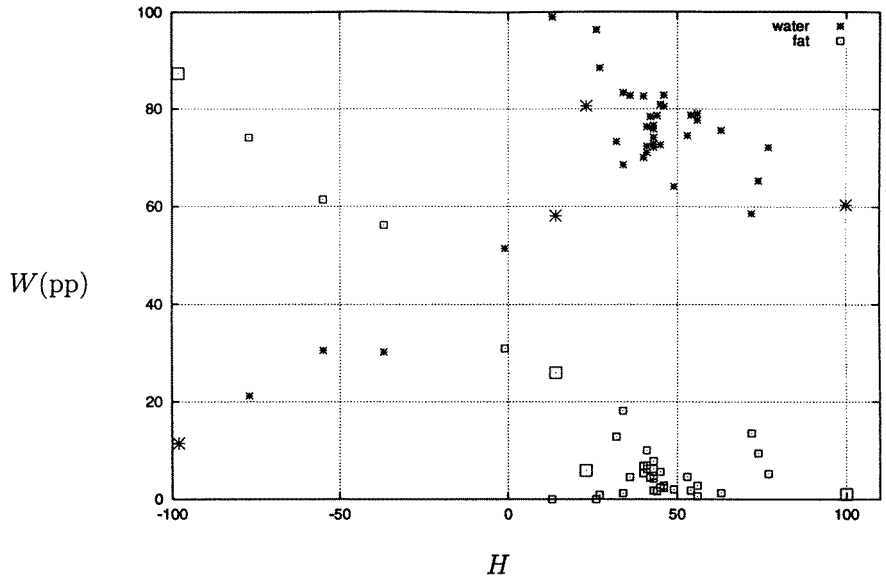

Figure 4. Weight proportions of water and fat in soft tissues versus Hounsfield units. The emphasized data points correspond to adipose tissue 3 ($H = -98$), adrenal gland ($H = 14$), small intestine (wall) ($H = 23$) and connective tissue ($H = 100$).

with

$$-22 \leqslant H \leqslant 1524.$$

In the latter equation, $w_{\mathrm{ma},i}$ and $w_{\mathrm{cb},i}$ denote the elemental weights of red/yellow marrow and skeleton cortical bone. Plots of functions (19) and (20) together with the data points for the

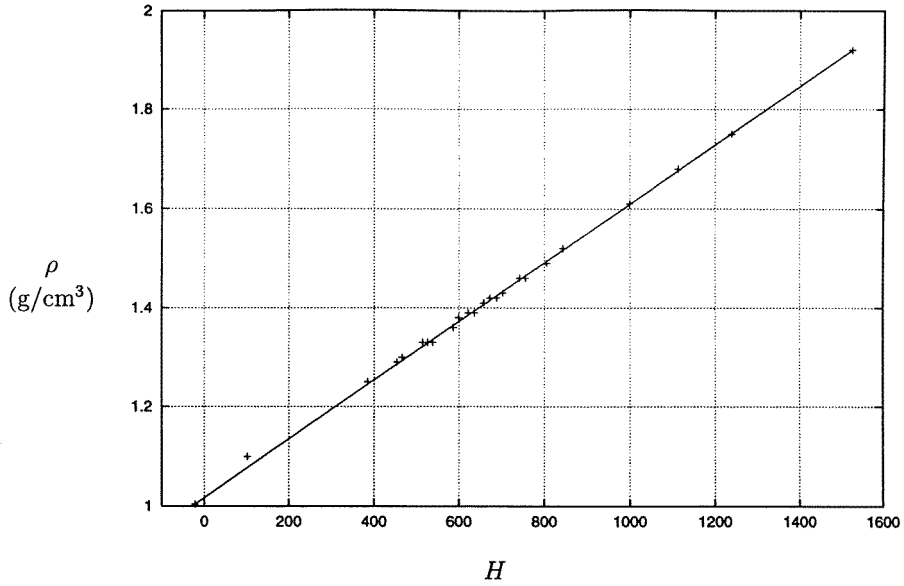

Figure 5. Mass density versus CT number in the range of skeletal tissues. The plot shows the data points of the skeletal tissues from table 5 together with the interpolation function (19).

skeletal tissues are shown in figures 5 and 6. By means of the interpolation function, the mass densities of all skeletal tissues are fitted with an accuracy better than 0.01 g cm^{-3}. Figure 6(*a*) shows that the weight of hydrogen is fitted with an accuracy of 0.2 pp (cartilage: 0.4 pp) and the weight of nitrogen with 0.7 pp. The weights of carbon and oxygen plotted in figure 6(*b*) are spread up to ± 9.7 pp around the interpolation functions. In case of cartilage, the deviation is even ± 38 pp. However, the data points of the sum of carbon and oxygen weights are well fitted using the corresponding interpolation function. The high spread of the individual weights on carbon and oxygen is due to the different proportions of red and yellow marrow in skeletal tissues. As can be see from table 5, the weights of carbon and oxygen in the two types of marrow differ by about 23 pp and 20.8 pp respectively. For the weights of phosphorus and calcium, the accuracy of the data fit is 0.2 pp and 0.6 pp respectively (cartilage: 0.6 pp/3 pp). Clearly, cartilage does not fit into the the composition model applied to skeletal tissues, therefore the big deviations are no surprise.

3.2. Data fit in the range of soft tissues

The interpolation functions for the fit of the data points of soft tissues are obtained by entering the data sets of (adipose tissue 3 (at), adrenal gland (ag)) and (small intestine (wall) (si), connective tissue (ct)) into formulae (17) and (18):

$$\rho = (1.018 + 0.893 \times 10^{-3} H) \text{ g cm}^{-3} \tag{21}$$

$$w_i = \frac{0.93(14 - H)}{114 + 0.1H}(w_{\text{at},i} - w_{\text{ag},i}) + w_{\text{ag},i} \tag{22}$$

with

$$-98 \leqslant H \leqslant 14$$

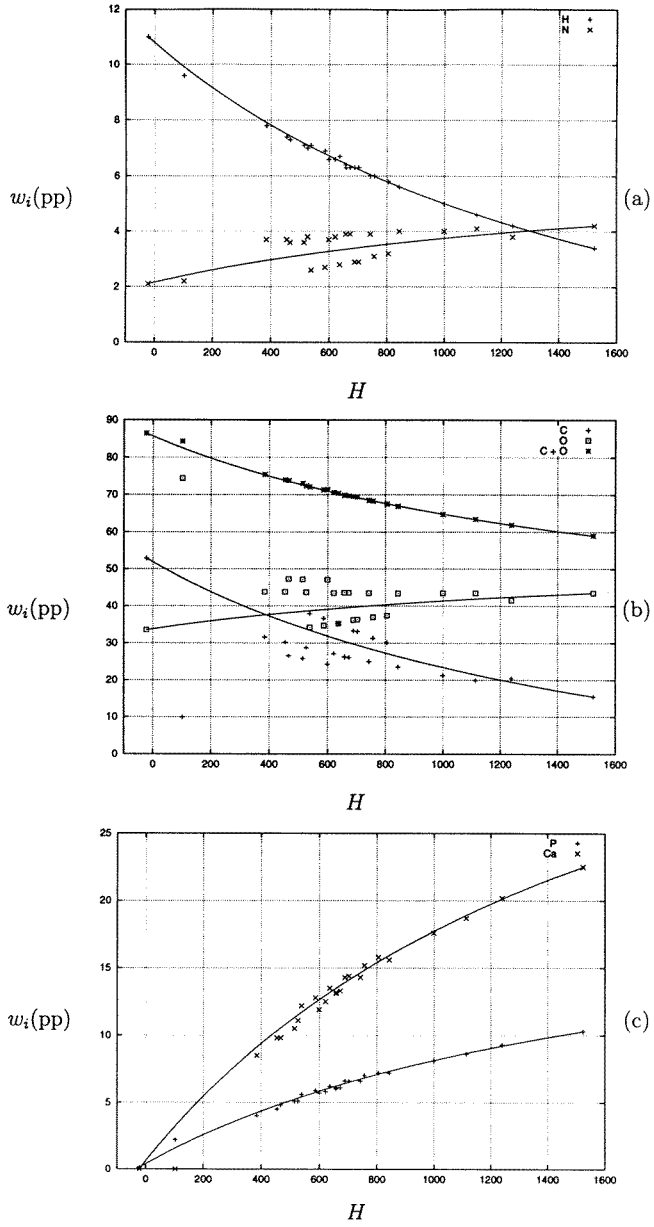

Figure 6. CT number versus elemental weights in the range of skeletal tissues. The plot shows the data points of the skeletal tissues together with the interpolation functions corresponding to (20): (*a*) hydrogen (H) and nitrogen (N), (*b*) carbon (C) and oxygen (O), (*c*) phosphorus (P) and calcium (Ca).

and

$$\rho = (1.003 + 1.169 \times 10^{-3} H)\ \mathrm{g\ cm^{-3}} \tag{23}$$

$$w_i = \frac{1.03(100 - H)}{77 + 0.09H}(w_{\mathrm{si},i} - w_{\mathrm{ct},i}) + w_{\mathrm{ct},i} \tag{24}$$

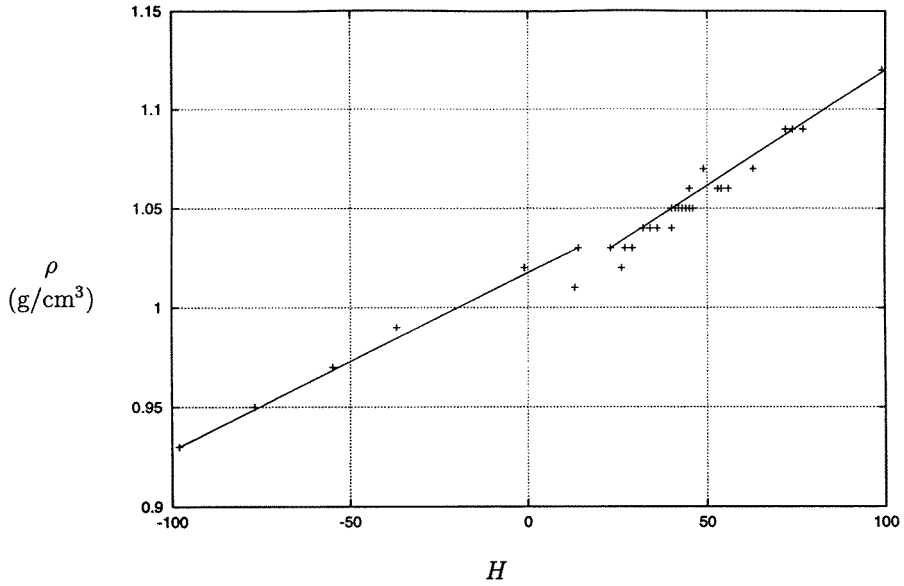

Figure 7. CT number versus mass density in the range of soft tissues. The data points of the tissues from tables 3 and 4 are plotted together with the interpolation functions according to formulae (21) and (23).

with

$$23 \leqslant H \leqslant 100.$$

Plots of the functions together with the data points for soft tissues are shown in figures 7 and 8. The data points of the mass density are fitted with an accuracy better than 0.01 g cm^{-3}. Only in the case of brain cerebrospinal fluid ($H = 13$) does a greater deviation occur (0.02 g cm^{-3}). For each of the elemental weights in the range between 23 and 100 Hounsfield units, we have calculated the mean deviation of the 35 data points to the fit values obtained by the interpolation functions. The mean deviation is then compared with the total spread of the data points. In case of hydrogen, the data points are distributed between 9.4 and 11.0 pp, whereas the mean deviation to function (24) is given by 0.2 pp. The minimum and maximum weights of nitrogen are 0.1 and 6.2 pp, the mean deviation of the data points to the interpolation function is 0.9 pp. Carbon and oxygen weights vary from 0.5 to 25.0 pp and from 59.4 to 86.2 pp respectively. The mean deviations of the data points to the interpolation functions are 4.2 pp for carbon and 4.6 pp for oxygen. In the range between -98 and 14 Hounsfield units lie the data points of only seven tissues. Clearly, brain cerebrospinal fluid ($H = 13$), on the border of the range, is not matched by the interpolation function. The weights of carbon and oxygen in mammary gland 1 ($H = -37$) deviate by 5 pp. For the weight of nitrogen, deviations of 0.7 pp occur in case of mammary gland 1 and 2. The remaining data points show only negligible deviations to the interpolation functions.

3.3. Conversion of the scale of Hounsfield units into tissue parameters

The results presented in the last section are not yet in a form suitable for use in Monte Carlo simulations. Codes like EGS4 offer the possibility of assigning to each geometrical region, i.e. to each CT voxel, a value for the mass density. On the other hand, the different tissue

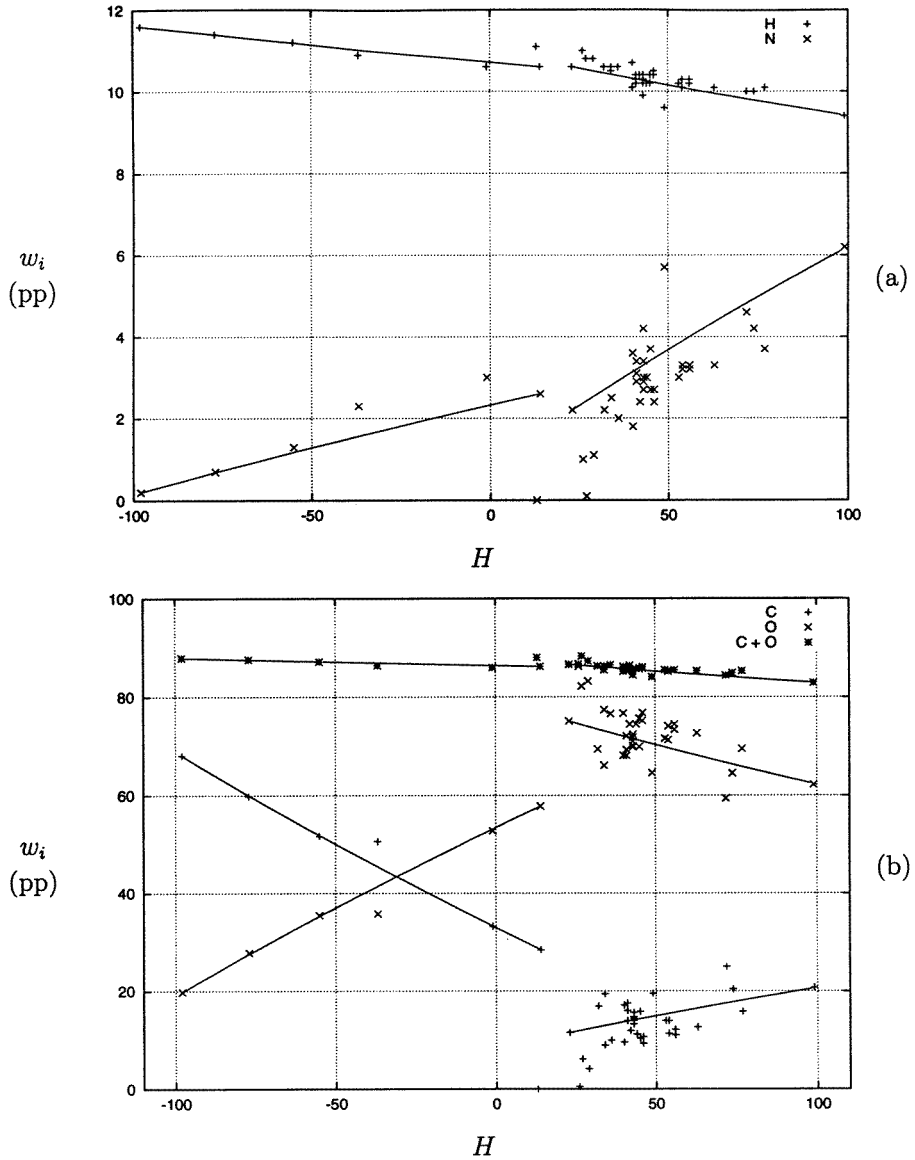

Figure 8. CT number versus elemental weights in the range of soft tissues. For each of the elements (*a*) hydrogen and nitrogen, (*b*) carbon and oxygen, the data points of the tissues from tables 3 and 4 are plotted together with the interpolation functions (22) and (24).

compositions have to be defined prior to the simulation. For each composition, a separate file including the cross sectional data has to be generated. Therefore, in case of the mass density, within the sections, the continuous correlation to the CT number can be used, whereas for the elemental weights a division of the full range of Hounsfield numbers into a number of bins has to be made. Figure 9 shows a plot of the conversion of Hounsfield units into mass density: Functions (21) and (23) are used for the range of soft tissues between −98 and 100 Hounsfield units. Within the gap on the scale of Hounsfield numbers between 14 and 23 units, a value of

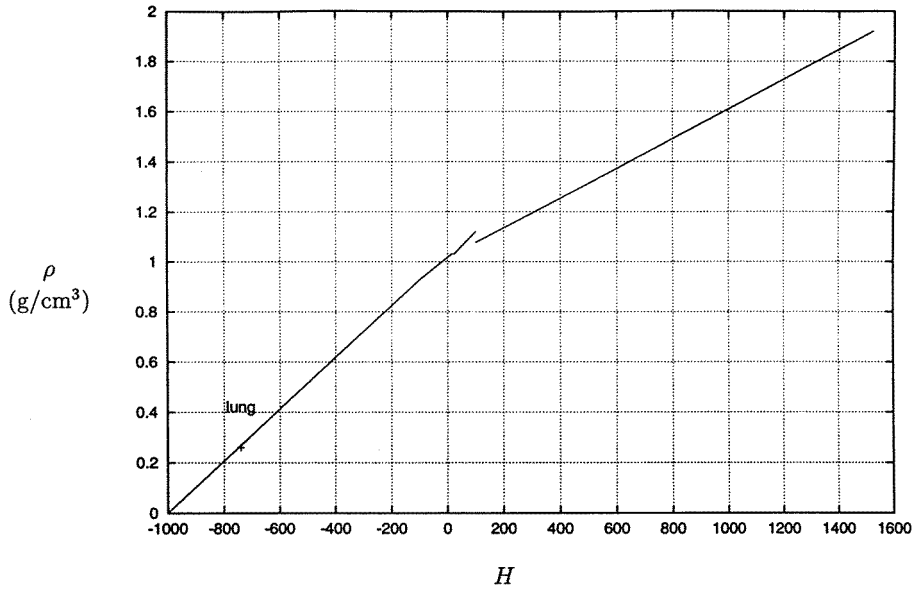

Figure 9. Conversion of CT number to mass density. Functions (21) and (23) are used for the range between −98 and 100 Hounsfield units. Above 100 H, function (19) is applied. In the range between −1000 and −98 H, the mass densities of air and adipose tissue 3 are interpolated by a straight line.

1.03 g cm^{-3} is used, causing no discontinuity. Function (19), which fits the skeletal tissues and which is defined for Hounsfield units greater then −22, is used only in the range above 100 H, because no skeletal tissue occurs below this value. There is a discontinuity of 0.04 g cm^{-3} at the transition from soft tissues to skeletal tissues. In the range between −1000 and −98 Hounsfield units, we interpolate the mass densities of air (1.21×10^{-3} g cm^{-3}) and adipose tissue 3 (0.93 g cm^{-3}) by means of a straight line. As can be seen from the plot, the mass density of lung is also well described.

To convert the CT number into the elemental weights, the continuous functional relationships $w_i(H)$ are transformed into step functions. To determine the step width, the following two points have to be considered. On the one hand, the smaller the step width the more cross sectional data files must be generated and the more data must be handled within the Monte Carlo simulation. On the other hand, with increasing step width, some of the available information about the elemental weights may be lost. It seems reasonable to determine the step width as big as possible with the constraint that the accuracy will not be substantially decreased by the binning. For that we have to consider the deviations ΔH between the CT numbers measured in the scanner and those calculated using formulae (6) and (10). The deviations of the determined elemental weights are limited to the corresponding ranges of values of all tissues having a calculated CT number within the range H(measured) $\pm\ \Delta H$. Our estimated values for ΔH are based on the deviations of the phantom materials used for the CT scanner calibration (see table 2). For the range of skeletal tissues, we assume a deviation of 50 Hounsfield units and define the bin width to 100 units. The maximum deviations which can occur are then as follows: hydrogen 0.8 pp, nitrogen 0.9 pp, carbon 11.8 pp, oxygen 9.9 pp, phosphorus 1 pp and calcium 2.3 pp. In the range of soft tissues between −98 and 14 H, we assume a smaller deviation of $\Delta H = \pm 15$ between measured and calculated CT numbers.

Table 6. Conversion of CT number to elemental weights. The scale of Hounsfield units is divided into 24 bins. The first bin from −1000 to −950 H is assigned to the composition of air, the next bin up to −120 H with the composition of lung. The following five bins up to 18 H form a step function corresponding to interpolation function (22). Between 19 and 80 H the mean values of all tissues within this range are used. The composition of connective tissue ($H = 100$) is assigned to the bin between 80 and 120 H. All bins above 120 Hounsfield units form a step function corresponding to interpolation function (20).

	w_i (pp)											
H	H	C	N	O	Na	Mg	P	S	Cl	Ar	K	Ca
−1000–−950			75.5	23.2						1.3		
−950–−120	10.3	10.5	3.1	74.9	0.2		0.2	0.3	0.3		0.2	
−120–−83	11.6	68.1	0.2	19.8	0.1			0.1	0.1			
−82–−53	11.3	56.7	0.9	30.8	0.1			0.1	0.1			
−52–−23	11.0	45.8	1.5	41.1	0.1		0.1	0.2	0.2			
−22–7	10.8	35.6	2.2	50.9			0.1	0.2	0.2			
8–18	10.6	28.4	2.6	57.8			0.1	0.2	0.2		0.1	
19–80	10.3	13.4	3.0	72.3	0.2		0.2	0.2	0.2		0.2	
80–120	9.4	20.7	6.2	62.2	0.6			0.6	0.3			
120–200	9.5	45.5	2.5	35.5	0.1		2.1	0.1	0.1		0.1	4.5
200–300	8.9	42.3	2.7	36.3	0.1		3.0	0.1	0.1		0.1	6.4
300–400	8.2	39.1	2.9	37.2	0.1		3.9	0.1	0.1		0.1	8.3
400–500	7.6	36.1	3.0	38.0	0.1	0.1	4.7	0.2	0.1			10.1
500–600	7.1	33.5	3.2	38.7	0.1	0.1	5.4	0.2				11.7
600–700	6.6	31.0	3.3	39.4	0.1	0.1	6.1	0.2				13.2
700–800	6.1	28.7	3.5	40.0	0.1	0.1	6.7	0.2				14.6
800–900	5.6	26.5	3.6	40.5	0.1	0.2	7.3	0.3				15.9
900–1000	5.2	24.6	3.7	41.1	0.1	0.2	7.8	0.3				17.0
1000–1100	4.9	22.7	3.8	41.6	0.1	0.2	8.3	0.3				18.1
1100–1200	4.5	21.0	3.9	42.0	0.1	0.2	8.8	0.3				19.2
1200–1300	4.2	19.4	4.0	42.5	0.1	0.2	9.2	0.3				20.1
1300–1400	3.9	17.9	4.1	42.9	0.1	0.2	9.6	0.3				21.0
1400–1500	3.6	16.5	4.2	43.2	0.1	0.2	10.0	0.3				21.9
1500–1600	3.4	15.5	4.2	43.5	0.1	0.2	10.3	0.3				22.5

The bin width is set to 30 Hounsfield units. The maximum possible deviations are: hydrogen 0.4 pp, nitrogen 1.4 pp, carbon 5.8 pp and oxygen 5.6 pp. In the case of mammary gland 1, the corresponding values for carbon and oxygen are ±15.4 pp. In the range of soft tissues between 23 and 100 Hounsfield units, the elemental weights are only weakly correlated with the CT number. We have therefore calculated for each elemental weight the mean value of all 35 soft tissues within this range. The mean deviations of the individual data points from the mean values are as follows: hydrogen 0.3 pp, nitrogen 1.2 pp, carbon 4.8 pp and oxygen 5.6 pp. These deviations are only slightly greater than the mean deviations of the data points from the fit values obtained using the interpolation functions (see section 3.2). Taking into account the deviations of the calculated CT numbers, a subdivision into different compositions within this range of soft tissues cannot significantly enhance the accuracy of the determined elemental weights. Therefore, we use the mean values instead of the interpolation functions. For connective tissue ($H = 100$), which is the soft tissue with the highest CT number, we have defined an individual bin. By definition, air has the CT number −1000. To consider statistical fluctuations in the CT data, all voxels with CT numbers lower then −950 are correlated with the composition of air. For the remaining range between air and soft tissues, we assign the composition of lung tissue, for which we have calculated −741 H.

4. Discussion

The difference in the CT numbers of most of the soft tissues is only small. Considering the limited reproducibility of the measured CT numbers and the only approximate formulae used for the calculation of the CT numbers, these tissues cannot be resolved by means of the CT number. Considering the mass density and the elemental weights of soft tissues, the greatest differences occur in the case of carbon and oxygen weights. This is due to the highly different contents of water ($w_C = 0$ pp, $w_O = 88.8$ pp) and adipose ($w_C = 77.3$ pp, $w_O = 10.9$ pp) in the individual soft tissues. To investigate the influence of different soft tissue compositions on Monte Carlo dose calculations, we have generated cross sectional data files using the mean elemental weights of the 35 soft tissues ($H > 24$) as well as using the elemental weights of two selected tissues namely urine and skin 1. For these tissues, the difference to the mean elemental weights are the greatest of all soft tissues. In case of urine, the deviations are H = +0.7 pp, C = −12.9 pp, N = −2 pp, O = +13.9 pp. The corresponding deviations for skin 1 are H = −0.3 pp, C = +11.6 pp, N = +1.6 pp, O = −12.9 pp. For a 2×2 cm^2 electron beam with 6 and 21 MeV, perpendicularly impinging a homogeneous cubic phantom with 20 cm side length, we have carried out Monte Carlo simulations with EGS4 based on each of the cross sectional data files. The mean composition was assigned with the mass density of urine and skin 1 respectively. For both energies, the differences between the resulting dose distributions of the mean composition and urine or the mean composition and skin 1 are lower than 1.6% of the maximum dose. In case of megavoltage photon beams, where Compton scattering is the predominant process, the influence of the individual weights of carbon, nitrogen and oxygen should be negligible. This is because the electron density depends only on the ratio of atomic number and mass, and this quantity is nearly the same for all three elements.

Within the range of skeletal tissues, the relative small estimated uncertainties, especially of the weights of the high atomic number elements phosphorus and calcium, justify a further subdivision into different compositions. Until now, however, only one mean bone composition has been used as input for Monte Carlo simulations. As in the case of soft tissues, we have investigated the influence of the elemental weights on Monte Carlo dose calculations. For that, we have generated cross sectional data files for a mean bone composition taken from Johns and Cunningham (1983) as well as for the skeletal tissues sternum and cortical bone. In case of the 6 MeV electron beam, the dose deviations between mean bone and sternum as well as between mean bone and cortical bone are 2.8% of dose maximum. For the 21 MeV electron beam, the dose values deviate up to 5.8% between mean bone and cortical bone and 3.8% between mean bone and sternum. The relatively big deviations are due to the different weights of calcium and phosphorus in skeletal tissues. In case of photon beams, the weights of both elements are not critical, because the ratio of atomic number and mass for calcium and phosphorus is the same as for carbon, nitrogen and oxygen. However, for hydrogen, this ratio is about a factor of two greater. Since the weight of hydrogen differs significantly between different skeletal tissues (sternum: $w_H = 7.8$ pp, cortical bone: $w_H = 3.4$ pp), the electron density can vary up to 3% depending on the hydrogen weight. This was not considered by du Plessis *et al* (1998), who have compared Monte Carlo dose distributions for a 8 MV photon beam using only one mean bone composition.

The necessity for a stoichiometric calibration of the CT number with physical quantities of tissues was mentioned by Schneider *et al* (1996). A shortcoming in their calibration procedure is that they have to carry out fits of all tissue data points. To take over their concept for the calibration of the mass density and all elemental weights seems to be very time consuming, in particular if one considers that the correlations between CT number and elemental weights are non-affine. Therefore, the method presented by us using interpolation functions between

selected tissues provides a substantial simplification of the procedure. Another advantage is that the elemental weights are already normalized to 100 percentage points.

5. Conclusions

In this paper, a method for a stoichiometric calibration of CT numbers with tissue parameters is presented. Compared with the method described by Schneider *et al* (1996), who had already established a stoichiometric calibration of CT numbers with electron densities and proton stopping powers, the application is now considerably simplified without loss of accuracy using the interpolation functions. The further advantage of our concept is that the non-affine relationship between CT number and elemental weights can be derived without having to perform non-affine fits.

Compared with the conversions of CT numbers into elemental weights, which are currently used in Monte Carlo algorithms for patient dose calculations, a much more detailed determination of the calcium, phosphorus and hydrogen weights in skeletal tissues can be obtained using our method. The results of Monte Carlo simulations have shown that the influence of calcium and phosphorus weights on the dose distributions of electron beams must not be neglected. The individual weights of carbon and oxygen in tissues are only poorly resolved by means of the CT number. Fortunately, the influences on the dose distributions are only marginal.

References

Constantinou C and Harrington J C 1992 An electron density calibration phantom for CT based treatment planning computers *Med. Phys.* **19** 325–7

DeMarco J J, Solberg T D and Smathers J B 1998 A CT based Monte Carlo simulation tool for dosimetry planning and analysis *Med. Phys.* **25** 1–11

du Plessis F C P, Willemse C A and Lötter M G 1998 The direct use of CT numbers to establish material properties needed for Monte Carlo calculation of dose distributions in patients *Med. Phys.* **25** 1195–201

Gao W and Raeside D E 1997 Orthovoltage radiation therapy treatment planning using Monte Carlo simulation: treatment of neuroendocrine carcinoma of the maxillary sinus *Phys. Med. Biol.* **42** 2421–33

Hartmann Siantar C L, Bergstrom P M, Chandler W P, Chase L, Cox L J, Daly T P, Garrett D, Hornstein S M, House R K, Moses E I, Patterson R W, Rathkopf J A and Schach von Wittenau, A 1997 Lawrence Livermore National Laboratory's PEREGRINE Project *UCRL-JC* 126732

Henson P W and Fox R A 1984 The electron density of bone for inhomogeneity correction in radiotherapy planning using CT numbers *Phys. Med. Biol.* **29** 351–9

Hogstrom K R, Mills M D and Almond P R 1981 Electron beam dose calculations *Phys. Med. Biol.* **26** 445–59

Jacob C 1997 Reichweite CT Zahl Beziehung von Phantommaterialien und Messungen mit einer neuentwickelten multisegmentierten Ionisationskammer zur Dosisverifikation bei Schwerionenbestrahlung *PhD Thesis* University of Heidelberg

Johns H E and Cunningham J R 1983 *The Physics of Radiology* (Springfield, IL: Thomas)

Kak A C and Slaney M 1988 *Principles of Computerized Tomographic Imaging* (New York: IEEE)

Kawrakow I, Fippel M and Friedrich K 1996 3D electron dose calculation using a voxel based Monte Carlo algorithm (VMC) *Med. Phys.* **23** 445–57

Kijewski P K and Bjärngard B E 1978 The use of computed tomography data for radiotherapy dose calculations *Int. J. Radiat. Oncol. Biol. Phys.* **4** 429–35

Manfredotti C, Nastasi U, Marchisio R, Ongaro C, Gervino G, Ragona R, Anglesio S and Sannazzari G 1990 Monte Carlo simulation of dose distribution in electron beam radiotherapy treatment planning *Nucl. Instrum. Methods* **291** A 646–54

Milan J and Bentley R E 1974 The storage and manipulation of radiation dose data in a small digital computer *Br. J. Radiol.* **47** 115–21

McCullough E C 1975 Photon attenuation in computed tomography *Med. Phys.* **2** 307–20

Nelson W R, Hirayama H and Rogers D W O 1985 The EGS4 code system *SLAC Report* 265

Parker R P, Hobday P A and Cassell K J 1979 The direct use of CT numbers in radiotherapy dosage calculations for inhomogeneous media *Phys. Med. Biol.* **24** 802–9

Rutherford R A, Pullan B R and Isherwood I 1976 Measurement of effective atomic number and electron density using an EMI scanner *Neuroradiology* **11** 15–21

Schneider U, Pedroni E and Lomax A 1996 The calibration of CT Hounsfield units for radiotherapy treatment planning *Phys. Med. Biol.* **41** 111–24

Wang L, Chui C-S and Lovelock M 1998 A patient-specific Monte Carlo dose-calculation method for photon beams *Med. Phys.* **25** 867–78

White D R, Woodard H Q and Hammond S M 1987 Average soft-tissue and bone models for use in radiation dosimetry *Br. J. Radiol.* **60** 907–13

Woodard H Q and White D R 1982 Bone models for use in radiotherapy dosimetry *Br. J. Radiol.* **55** 277–82

——1986 The composition of body tissues *Br. J. Radiol.* **59** 1209–19